Decentralized Voltage Control Strategies for Microgeneration in Low-Voltage Distribution Grids

Digest of the Thesis to obtain the Master of Science Degree in Electrical and Computing Engineering

by João C. Botas de Campos, Universidade de Lisboa, IST - MEEC, 2016

Supervisor: Prof. Pedro Manuel dos Santos Carvalho

***Abstract* — Due to the expansion of distributed generation (DG), decentralized voltage control has been gaining traction as the leading strategy for the regulation of distributed energy resources (DERs) in low-voltage (LV) networks. However, this methods carries several, often overlooked, drawbacks that can compromise these grid's voltage profile. In this thesis, we model several reduced circuit networks and a basic control algorithm, then expounding upon the issues of system instability and restrictions on the DERs' power output. By managing each controller's power gain, an alternating power controller is then put forward and simulated, after which the base network model is expanded upon. An alternate voltage error integration controller is lastly proposed, ameliorating the unpredictability of the error due to an unbalanced distribution of DERs. This thesis ultimately concludes that a decentralized control strategy, while feasible, cannot be applied in real-life without a much more in-depth study on its limitations.**

***Index Terms* — distributed energy resources, decentralized voltage control, system instability, alternating power controller, controller power gain, voltage error integration.**

I. Introduction

Microgeneration has been steadily rising in prominence over the past two decades, and it's reasonable to expect that it will continue to expand over the foreseeable future, particularly in developed countries [1]. The advent of smaller and affordable photovoltaic (PV) panels [2] has resulted in the considerable growth of scaled-down generation sites, located downstream in low-voltage (LV) electric networks. This trend has raised several pressing concerns within the pertaining academia seeing that most of the current distribution network's infrastructure wasn't conceived with a large concentration of distributed generation (DG) clusters in mind [3].

The primary matter of contention relates to voltage rise, caused by the inversion of the regular power flow due to a significant number of installed DERs [4]. This is particularly relevant in situations where the reactance-to-resistance ratio is small, such as is the case with LV distribution networks. This unwanted deviation in the network's voltage profile comes as a consequence of the inversion of the regular power flow, caused by the substantial injection of active power into the grid by the connected DG. The network's functionality can thus be compromised as result, moreso when taking into account the problem of voltage cascading [5].

Centralized control strategies, through which the profile would regulated by distributed network operator (DNO), have been proposed to counteract these situations. However, due to its unreliability and high cost, its decentralized counterpart has been gaining traction as a more practical alternative [6]-[8]. With it, each local DER controller would autonomously regulate its injected power in order to maintain its nodal voltage within a fixed set-point, without any sort of external input. But while advantageous, the widespread adoption of this type of voltage control poses its significant share of underlying drawbacks, of which there's a somewhat startling lack of effort to address. The most egregious of these pertains to a possible instability of the overall control algorithm, that is a divergence of the voltage error, not wholly avoidable without an overseeing master controller. Another concerns, the physical limitations of the equipment, which will place restrictions on power output, in tandem with present environmental conditions.

In this work, we aim to demonstrate the large degree of frailty the decentralized control process has in terms of its stability, when pressed by the myriad of factors that affect a feeder network. Namely, demonstrating how easily the it is influenced by the number and distribution of the DERs, among other factors, as it's extensively documented [9]. Concurrently, we also strived to put forward and properly experiment with an adequate theoretical voltage control scheme, as part of a wider strategy to consign micro-producers as voltage regulators, that can (at least partially) counteract these flaws.

The paper is organized as follow. In Section II, we define the basic network and algorithm model to be used throughout the work. In Section III, we showcase, and try to work around, its limitations in terms of algorithm convergence and injected power output. Section IV concerns the simulation results of the presented system. In Section V, the base grid circuit is further expanded upon, in order to study the system under more realistic conditions. In Section VI, an integral area based alternative controller is presented, as a means to counteract many of the previously presented faults. Finally, in Section VII we conclude this paper.

II. Decentralized System Modelling

A. Low-Voltage Network Outline

The modeling of LV networks behavior under unbalanced load and generation conditions requires a four-wire (three-phase and neutral) full circuit representation. However, a proxy of the impedance matrix can be easily built for the nodes of interest based on cable ohmic characteristics and topology inspection [10]. Such impedance matrix encloses sufficient information to analyze voltage control algorithms as it represents the sensitivities of nodal voltages w.r.t power injections [5].

In this thesis, we model several systems response to voltage control of single-phase connected DER with such a matrix. Two of those cases, models 6 and 9, are displayed in Fig. 1, representing the positioning of the three generators in the 3bus-by-3phase grid.

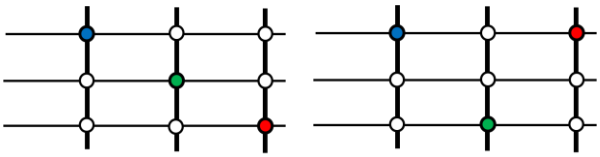

Figure 1. LV grid diagrams with three generators, one per phase (left – study model 6) and two on the same phase (right – sutdy model 9).

Let us refer to the proxy of the impedance matrix by $R + jX$ and approximate the relationship between the voltage drop ΔV and the variation of the net active ΔP_G and reactive ΔQ_G power generation in each node through

$$[\Delta V] = [R]([\Delta P_G] + x{\circ}r\,[\Delta Q_G]) \qquad (1)$$

where, the term $x{\circ}r$ represents the reactance-to-resistance ratio, assuming it is constant throughout the entire grid, and R is the grid's n-by-n (n being the number of connected generators) resistance matrix.

Assuming that the bus impedance between nodes is roughly the same both for the phase and neutral conductors, R can be written as:

$$R_{ij} = \begin{cases} R_{ij}^{el} & if\ i\ and\ j\ are\ in\ phase\ (p) \\ -1/4\, R_{ij}^{el} & otherwise \end{cases}. \qquad (2)$$

where R_{ij}^{el} stands for the *smallest* loop resistance between i and j, as in source-to-node trough p and then node-to-source trough the neutral.

Assuming the internodal resistance is of 0.2 pu (base 100kVA for 400V), plus 0.4 pu between the source and the most upstream bus, we get the following impedance matrixes for the feeders of Fig.1, which we will be later using in our simulations.

$$R_6 = \begin{bmatrix} 0.8 & -0.2 & -0.2 \\ -0.2 & 1.2 & -0.3 \\ -0.2 & -0.3 & 1.6 \end{bmatrix},\ R_9 = \begin{bmatrix} 0.8 & -0.2 & 0.8 \\ -0.2 & 1.2 & -0.3 \\ 0.8 & -0.3 & 1.6 \end{bmatrix}.$$

B. Decentralized Controller Logic

As [5] describes it, this iterative process can be summed up as in Table I.

Table I: Logical steps of a Voltage Dependent Q(V)/P(V) controller

Step 1	Compare set-point V^* and actual voltage to obtain error: $\Delta V_i = V^* - V_i$;
Step 2	Compute power-shifts ΔP_i and ΔQ_i based on ΔV_i and gains: $\Delta P_i = k_P \Delta V_i$, $\Delta Q_i = k_Q \Delta V_i$;
Step 3	Update V_i based on the new values of P_i and Q_i: $V_i = f([P_i, Q_i])$;
Step 4	Check if $V_i \neq V^*, \forall_i$: If True → return to Step 1; Else → stop;

Accordingly, the control and state equations concerning Step 2 and 3 are, respectively, given as

$$p^{k+1} = p^k + [k_P](V^* - V^k) \qquad (3.1)$$
$$q^{k+1} = q^k + [k_Q](V^* - V^k) \qquad (3.2)$$
$$V^{k+1} = V^k + [R]((p^{k+1} - p^k) + x{\circ}r(q^{k+1} - q^k)) \qquad (4)$$

where k_P and k_Q represent the active and reactive power gains w.r.t. to the nodal voltage of each DER. By combining the three above equations, we can surmise the voltage update formula as:

$$V^{k+1} = ([I] - [R][k])V^k + ([R][k])V^* \qquad (5)$$

where $[I]$ is a n-by-n identity matrix and $[k] = [k_P] + x{\circ}r[k_Q]$, which we will designate as the overall gain matrix. We can evaluate the convergence of this update formula through the eigenvalues of the matrix that serves as the coefficient for the last obtained iterative term V^k, which we will designate as $[A] = [I] - [R][k]$. Per [16], the stability conditions for such process are met *iff the absolute values of the eigenvalues of* $[A]$ *are all less or equal to one*. Furthermore, if said values are also non-negative and real the system will converge in a non-oscillatory manner, returning to its steady state through exponential decay of the error.

$$A(R_6) \rightarrow \lambda = \{-.7683\ ;\ -.2121\ ;\ -.3804\}$$
$$A(R_9) \rightarrow \lambda = \{-1.2215\ ;\ -.0731\ ;\ -.6946\}$$

The above eigenvalues indicate that, with an unitary gain matrix $[k] = [I]$, the error behavior will be oscillatory for model 6 and unstable for 9. In this state, the algorithm will not converge to its set-point in an admissible manner for nearly all of the network schemes. In order to mitigate this liability the algorithm has to update its injected power more conservatively through an attenuation factor, thus enabling its convergence. As $[R]$ is a fixed value, it falls upon the overall gain matrix $[k]$ to act as the attenuator, allowing us to lessen the difference between the power values in-between iterative steps.

This value can be rewritten as $[k] = \alpha[K]$, where α is the common (network-wide) gain factor, of which the eigenvalues of $[A]$ are linearly dependent, and $[K]$ is the controller specific gain. This latter will define $[k_{stb}]$, which is the limit power gain of the system, as $Max|\lambda(A([R.k_{stb}]))| = 1$, putting the system at the threshold of instability. As we can comparatively measure a system's robustness basing ourselves on this value, defining which $[K]$ to use in each controller becomes critical.

III. Limits to Fully Decentralized Voltage Control

A. Controller Power Gain through Inverse Impedance

Now aware of the theoretical weight of $[R]$ and $[K]$ on the system's stability, the next step will be to define the individual controller's power gains. To avoid issues that would arise due to the spacing of the DERs, we chose to base these values on the inverse impedance "seen" by each controller. This results in $[K] = [R_I]$, where the latter is the inverse matrix of the diagonal of $[R]$, again reflecting the lack of information between generating nodes and the closest approximation to the ideal $[R]^{-1}$ (that would yield $[A] = [I] - [R][R]^{-1} = 0 \rightarrow \lambda(A) = 0$). Adopting this strategy, models 6 and 9 yield:

$$R_6 \rightarrow [k_{stb}] = \{2.044\,;\ 1.363\,;\ 1.022\}$$
$$R_9 \rightarrow [k_{stb}] = \{1.377\,;\ 0.918\,;\ 0.689\}$$

The core issue pertaining to the stability of a decentralized control scheme revolves around the influence between the various DERs connected throughout a feeder grid and an inherent lack of information available to their controllers. The most logical workaround would then be to eliminate this simultaneity, ensuring that only one controller updates at any given time. This would result in a triangular matrix $[A]$, whose eigenvalues would be equal to $1 - R_{ii}k_{ii}$ and 1, ensuring the system's stability so long as $R_{ii}k_{ii} \leq 2$. While with a discrete decentralized controller, this would be hard to implement, later ahead we'll be seeing a alternative control strategy that makes use of this.

B. Limitations on Injected Power

While capable, in theory, of solving any divergence in the voltage profile, if the stability criteria are met, the physical aspects of the electrical equipment will place other restrictions upon the system. The two main cap factors are the available active power P_A, defined by the quantity solar irradiance collected by the PV panel, and the generator's overall capacity to inject reactive power. This latter will define an operational area for the DER in the form of a semi-circle in a $[P, Q]$ plane with a radius of S_M, its maximum apparent power. Due to this value, the following stipulation will be imposed:

$$S_M{}^2 \geq P_G{}^2 + Q_G{}^2 \tag{6}$$

whereas $0 \leq P_G \leq P_A$. Because of these limits, there is now a possibility that the state variable will not be able to converge to the intended set-point. As such, it becomes necessary to weigh in the initial conditions of the system when the controller is activated, specifically the voltage and power values at the beginning of the controller's iterative sequence. Taking (4) into account, we can define P_f and Q_f as the two power components' values at the end of a successful iterative process. If we're to assume that the system became bounded to the limit curve, we have that:

$$V^* - V^0 = R\left(P_f - P^0 + x \circ r\left(Q_f - Q^0\right)\right), \quad with\ \ Q_f = \sqrt{S_M{}^2 - P_f{}^2}. \tag{7}$$

Solving for P_f, we get:

$$P_f = \frac{\frac{C_0}{x \circ r} \mp \sqrt{\left(1+\frac{1}{x \circ r^2}\right) S_M{}^2 - C_0{}^2}}{\left(1+\frac{1}{x \circ r^2}\right)},\ C_0 = \frac{R^{-1}(V^* - V^0) + P^0}{x \circ r} + Q^0 \tag{8}$$

And seeing as P_f has to be a real number:

$$\sqrt{(1 + x \circ r^2)}\, S_M - |R^{-1}(V^* - V^0) + P^0 + x \circ r\, Q^0| \geq 0 \tag{9}$$

If the inequality holds, in addition to $\min\{p_{f1}, p_{f2}\} \leq P_A$, then the state variable is fully capable of converging to its set-point V^*, since a set of coordinates $[P_G, Q_G]$ exists within the established boundaries. Moreover, from (8) we can determine that there're possibly two solution sets of power coordinates in the limit curve. From these two point, we can trace a line in the $[P, Q]$ plane, whose equation can be taken from (7):

$$Q_f(P_f) = C_0 - x \circ r^{-1} P_f \tag{10}$$

It stands to reason then that all points contained in (10), and (6), are all valid solutions for the voltage error enclosed in C_0. This allows for some considerable leeway seeing that the network's voltage profile will remain undisturbed so long as the injected nodal power "travels" along the line defined by (10). In fact, any line with a $-x \circ r^{-1}$ slope will contain the all the power coordinates for one specific voltage profile, and with each iterative step we consecutively jump between several of these parallel lines, progressively closing in on (10). Those tangent to the limit curve (7) represent the highest attainable positive and negative shift in the DER's voltage, leading to another inequality that also needs to be valid, in tandem with (9):

$$S_M\, x \circ r^{-1}(1 + x \circ r^2)^{1/2} \geq C_0 \geq -S_M \tag{11}$$

C. Updated Control Algorithm

Given P_A and S_M, it's evident that the control algorithm in Table I will need to suffer several modifications to take in account these two new restricting parameters to its operation. Specifically, we chose to have only a single type of voltage dependent control operate at a time, meaning having either $[k] = [k_P] + 0$ or $[k] = 0 + x \circ r[k_Q]$, alternating between them as necessary. As we want to avoid a drop in the injected active power, we gave $Q(V)$ precedence over its counterpart. Furthermore, we also introduced some degree of foresight to the controller, so that it doesn't become bound to the limit curve. The updated logic is illustrated in Fig. 2 and described in Table II:

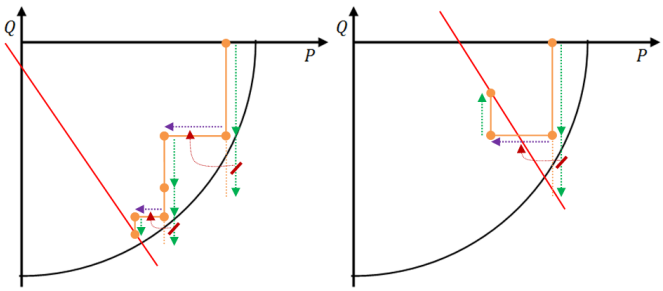

Figure 2. [P, Q] plane hypothetical representations the logical steps taken by the controller when correcting an instance of nodal voltage deviation, when using an the foresight strategy. Green vertical arrows represent Q(V), purple horizontal arrows P(V) and the red line the solution set of values per (10).

TABLE II: LOGICAL STEPS OF A VOLTAGE DEPENDENT Q(V)/P(V) CONTROLLER, WITH Q(V) PRECEDENCE AND FORESIGHT

Step 1	Compare set-point V^* and actual voltage to obtain error: $\Delta V_i = V^* - V_i$;
Step 2	Compute power-shift ΔQ_i based on ΔV_i and gain: $\Delta Q_i = [k_Q]_{ii}\Delta V_i = x \text{ or}^{-1}[k]_{ii}\Delta V_i$; Check if ${S_M}^2 \geq {P_i}^2 + (Q_i + \Delta Q_i)^2$
Step 3	If True → continue to Step 4; Else → Compute power-shift ΔP_i based on ΔV_i and gain: $\Delta P_i = [k_P]_{ii}\Delta V_i = [k]_{ii}\Delta V_i$, and discard Step 2's ΔQ_i;
Step 4	Update V_i based on the new values of P_i or Q_i: $V_i = f([P_i, Q_i])$;
Step 5	Check if $V_i \neq V^*, \forall_i$: If True → return to Step 1; Else → stop;

IV. SIMULATION RESULTS

A. Voltage Error Behavior and System Performance

Before the error behavior and system performance can be simulated, we'll first need to establish a set of initial values for the nodal voltages of each grid configuration. As we'll want them to represent a more or less realistic scenario, that could be encountered in any practical feeder network, we made use of a simple power-flow MATLAB code to calculate a satisfactory set of values for the initial error. The results yielded by the simulation are:

$$R_6 \rightarrow V^0 = \{1.1174;\ 1.1126;\ 1.1227\}$$
$$R_9 \rightarrow V^0 = \{1.1179;\ 1.1135;\ 1.1252\}$$

For a first behavior study, we'll ignore all of the initial power conditions and restrictions, focusing solely on voltage error, with a set-point $V^* = 1.1$. Furthermore, as to compare the error's overdamped and oscillating behavior respectively, for the left graphs we'll have a $[k] = .475[k_{stb}]$, as the oscillatory threshold is half of the instability's, and for the right $[k] = .975[k_{stb}]$. We'll also take note the speed of the algorithm, i.e. the number of iterations it takes for the maximum voltage error to drop below a certain value, in this case 10^{-4}, even if it's beyond the displayed 20 iterations.

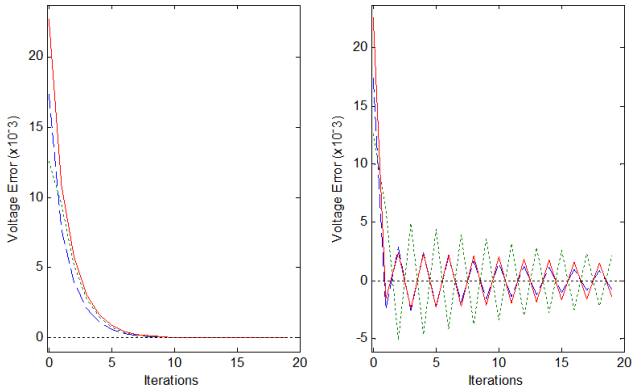

$Lag \rightarrow 9$ $Lag \rightarrow 79$

Figure 3. Evolution of the state variable error for study model 6, with $[k] = .475[k_{stb}]$ (left) and $[k] = .975[k_{stb}]$ (right), up to 20 iterations. Below each graph is the number of iterations until $max|V_i - V^*| \leq 10^{-4}$.

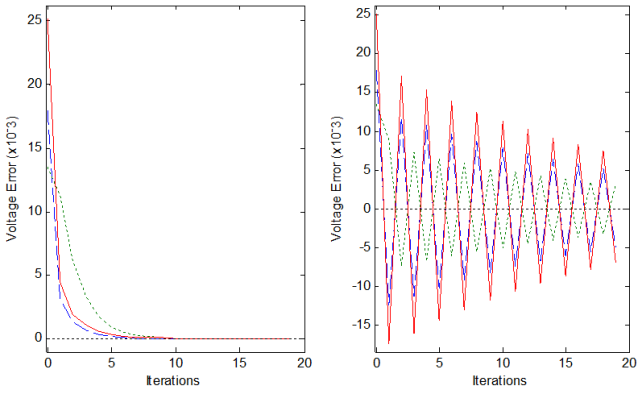

$Lag \rightarrow 9$ $Lag \rightarrow 103$

Figure 4. Evolution of the state variable error for study model 9, with $[k] = .475[k_{stb}]$ (left) and $[k] = .975[k_{stb}]$ (right), up to twenty iterations. Below each graph is the number of iterations until $max|V_i - V^*| \leq 10^{-4}$.

As predicted, with the given overall power gains, the generators managed to successfully correct their own voltage error, relying solely on their own autonomous control system. In the left graphs, we notice that when the both systems are overdamped, and despite the dissimilar initial voltage values, all error curves tend to coalesce together, approaching V^* at the same rate after the first few iterations. The algorithm's lag is also equal for these, likely owing the slight differences in V^0 for each model. However, despite this very fact, for $[k] = .975[k_{stb}]$ the speed with which the error amplitude decays is much more visibly distinct for each configuration.

Though not noticeable with the two chosen models, given the remainder we can take other conclusions pertaining to the nodal voltage. Overall, with an unbalanced distribution of the DERs through the three phases, it takes a greater amount of time for the algorithm to correct a network's profile deviation Another, it's that its average initial error tends to be greater in situations with unbalance distribution of loads, due to the addition of a mutually induced increase for same-phase nodal voltages. In addition, the disparity between the voltage in the three nodes tends to be more pronounced when they're clustered together.

Matrix-wise, the greater the difference between the magnitudes of a matrix's diagonal and the sum of their respective non-diagonal terms (diagonal dominance), the faster the algorithm will be able to correct the voltage error for the corresponding configuration. Seemingly minute difference in configuration can cause significant differences in both behavior and performance, which is in line with our previous conclusion that the algorithm's efficiency is directly correlated with the influence each DER exerts on one another: the lesser the better.

Another question one could ask, based on what was seen above, is what specific α can provide the best speed for each system. Again through simulations, we've found the range of gains that produce the fewest iterations for the two models:

$$R_6 \rightarrow [\ .600\ ,.755\ ] \times [k_{stb}] \rightarrow lag = 6$$
$$R_9 \rightarrow [\ .605\ ,.685\ ] \times [k_{stb}] \rightarrow lag = 6$$

while, with all the other models in mind, $[k] = 0.75[k_{stb}]$ appears the best universal compromise.

B. *Active and Reactive Power Curtailment*

While the chosen controller power gain will have an effect on the difference between initial and final values, the solution set is ultimately the same regardless, seeing that C_0 is independent of $[k]$. This means that the power gain only determines where in line (10) the controller ends up in, and as such we can always readjust the coordinates to fit any criteria we wish. This can be done with each iteration, as moving along a $-x \circ r^{-1}$ slope line does not change the voltage profile, or at the very end of the process. As we'll want to curtail the drop in active power first and foremost, and to demonstrate this property of (10), we'll showcase the latter as to obtain the lowest possible ΔP. Therefore, each final value in the following graphs represent the minimal variations of active power necessary to correct the deviation, with $p_0 = 0.95$ and $q_0 = -0.3$.

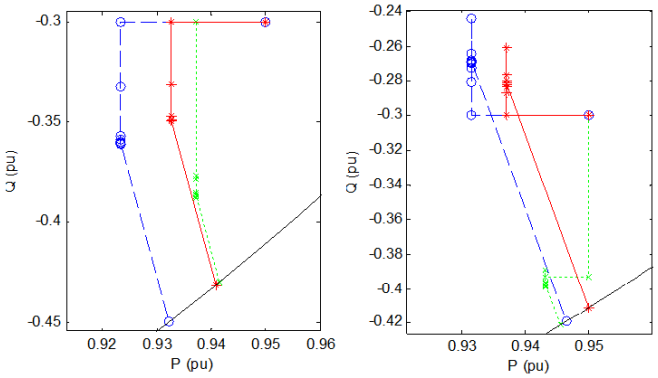

Figure 5. Evolution of the control variables for study model 6 (left) and 9 (right), with $[k] = .75[k_{stb}]$, up to a hundred iterations. At the end of the iterative process, a last readjustment along each respective (10) was made to minimize ΔP. In both these final shifts, the network's voltage profile remains unchanged, similarly as to those exemplified in Fig. 3 and Fig. 4.

And the final values for the injected power:

Model 6	
$\Delta P_1 = -.0178$	$\Delta Q_1 = -.1496$
$\Delta P_2 = -.0085$	$\Delta Q_2 = -.1300$
$\Delta P_3 = -.0092$	$\Delta Q_3 = -.1314$
$\Delta P_{total} = .0355$	$\Delta Q_{total} = .4110$

Model 9	
$\Delta P_1 = -.0035$	$\Delta Q_1 = -.1187$
$\Delta P_2 = -.0045$	$\Delta Q_2 = -.1210$
$\Delta P_3 = -.0001$	$\Delta Q_3 = -.1110$
$\Delta P_{total} = .0081$	$\Delta Q_{total} = .3507$

It's immediately observable that for study model 9 the total power shift, both active and reactive, is less than that required for model 6, despite sharing a very similar V^0 and DER configuration. The same holds true for every model with more than one generator per phase in comparison to those with only one, even when the general initial voltage error for the former is greater or roughly equal than the latter's.

This occurs because any change in the nodal voltage of a DER, rise or fall, will produce an identical response along the line. Thus, because of the way the DG network is configured, same phase-connected generators will mutually help each other eliminating their overvoltage, generally lessening the needed decrement in injected power for each one. In turn, this also abates the induced voltage hike in the other two-phases, allowing for a similarly smaller power shift to correct the deviation as the controller no longer has to compensate as much for said increase. However, this can also work against the system, as when same-phase nodes have opposite error signals necessitating then an *increase* in the injected power, which can naturally be problematic given the set restrictions.

Moreover, we saw that by using the properties of (10) we can also manipulate the injected power to better suit our needs, whether it be to minimize ΔP (or ΔQ instead), fix Q/P to a certain ratio, or even the set a desired power factor. More importantly, the trace it leaves allows to ascertain the relative positioning of each generators' solution set for the given initial parameters. It also permits a more accurate gauging of the relative shifts in active power, independent of the chosen gain, as it will always lead to the same results regardless of $[k]$.

V. Expanding the Study Model

A. *Concentrated Generation*

Though we in previous Section we verified the feasibility of the decentralized voltage control strategy, at the same time we've also ascertained how the initial conditions for voltage (V^0) and injected power (p^0 and q^0) can affect this process, possibly even precluding it. Same goes for the configuration sensible eigenvalues that dictate whether or not the system is stable. It's within reasonable expectation that any feeder network in real life will have a higher number of generators injecting power into it than the three we've worked with so far, with different patterns of distribution. Thus, it becomes imperative for our study to expand the LV circuit model, to analyze the impact on the behavior of the control and state variables as the resistance matrix $[R]$ is gradually morphed and, more crucially, the viability of the autonomous control scheme as it does.

First we'll evaluate what occurs when we gradually 'fill' the nine node circuit grid, from three DERs to six, then to nine. To assess the relative stability between each case, we'll again resort to comparing the diagonal terms of the maximum stability overall gain matrix $[k_{stb}]$. Due to the number of possible combinations for generator distribution, we elected to pick the worst possible cases for each configuration, being those that generates the highest possible $|\lambda_i|$. The results were as follow:

$$3 \text{ DERs} \rightarrow [k_{stb}] = 0.7707[K]$$
$$6 \text{ DERs} \rightarrow [k_{stb}] = 0.6166[K]$$
$$9 \text{ DERs} \rightarrow [k_{stb}] = 0.6166[K]$$

It is not at all surprising to observe that a higher number of connected DERs invariably leads to a necessary decrease in the overall gain to assure the system's stability, yet another indication of its precariousness in relate to the generators. This cut results from the overarching algorithm struggling to juggle and consolidate the power flow of more generators in order to maintain an adequate voltage profile. Interestingly, it also seems that maximum gradient caps off when two of the phases are completely filled, starting with upwards of six DERs. Ultimately, the inclusion of more DERs ultimately means more possible grid configurations, which in turn means more ways that each generator play off each other, exacerbating all of these concerns as we strive predict what kind of ripple effects might originate from such scenarios.

One of such issues pertains to the system's performance. As the system juggles with an increasing number of DERs, and thus an equally growing number of added elements to the network's power flow, it's natural to assume that the speed with which it can resolve any of these deviation will tend to lower, as seen above. However, such assumption may not be as straightforward as it initially appears. To showcase this intrinsic complexity, we've repeated the same simulations for 3+ DERs, this time with the intent of obtaining the number of iterations the system requires so that $max|V_i - V^*| \leq 10^{-4}$, for $\alpha = 0.3$ ($[k]$ near the oscillation threshold) and $\alpha = 0.6$ ($[k]$ near the stability threshold).

TABLE III: INITIAL VALUES FOR THE NODAL VOLTAGE AND SUBSEQUENT SYSTEM PERFORMANCE

Number of DERs	V^0	lag	
		$\alpha = 0.3$	$\alpha = 0.6$
3	$\{1.0933; 1.1277; 1.1390\}$	122	60
6	$\{1.1032; 1.1217; 1.1351\}$ $\{1.1045; 1.1226; 1.1330\}$	80	37
9	$\{1.1230; 1.1203; 1.1168\}$ $\{1.1243; 1.1212; 1.1199\}$ $\{1.1196; 1.1191; 1.1157\}$	96	64

A cursory glance at the results indicates that, while do we notice a change in the system's performance with an increase of generation, it doesn't appear to be proportionally related with the amount of generators in operation. As we suspected, it's not the actual number of DERs that influences the speed with which the controlling algorithm can correct disturbances in the network's voltage profile. The speeds between each setup seem to own their dissimilarity to a variety of factors, not least of which being the initial values for the nodal voltage, both in magnitude and in disparity between one another.

Upon subsequent examinations, we can conclude that when the error in one or more nodes is fully eliminated or significantly reduced while that of the others remains relatively higher. The controllers pertaining to the former, in an attempt to keep their nodal voltages mostly fixed, will act as a sort of anchor for the system, thus slowing it down. Mathematically, $[A]$ is effectively reduced in size, increasing the maximum common gain factor α. This *anchoring* phenomenon caused by one of the controller's reaching its end goal ahead of its companions also explains why an oscillatory response is preferable (in terms of speed) to an overdamped reduction of the error.

B. Dispersed Generation

Previously, we demonstrated how the superficially simple matter of adding an extra generator or simply readjusting one's position in the feeder grid can lead to drastic changes in both performance and stability wise. Having seen the effects of concentrating generation, we'll now observe the opposite, that this measuring what influence distance – the impedance $R_{ii}(1 + j\,x\circ r)$ seen by each individual DER and its $R_{in}(1 + j\,x\circ r)$ derivatives – has on the 3bus-by-3phase node grid.

As one would've expected, preliminary simulations have confirmed that accruing the line impedance between the generating busses does improve the stability limit. However, despite upwards of a hundred times its original value, this increase in intermodal resistance does not result in an equally significant improvement. Ideally, and supposing one DER per bus, if the generating busses were properly isolated from one another, then the following generalization could be made for $[A]$:

$$[A] \approx \begin{bmatrix} 1-\alpha & 0 & 0 \\ -\alpha/4 & 1-\alpha & 0 \\ -\alpha/4 & -\alpha/4 & 1-\alpha \end{bmatrix} \Rightarrow [k_{stb}] = 2[K]$$

However, we can only make this simplification when the ratio between the impedances seen by adjacent busses tends towards zero as the distance between them increases. While this is true for the two busses closest to the source, the same cannot be said between the two farthest from it. Therefore, to make use of the distance to our benefit we'll have to increase the *relative distance* between the generating busses rather than simply adding identical increments. One possible solution, as an example, would be to distance the busses by a logarithmic factor instead, as seen in the figure below:

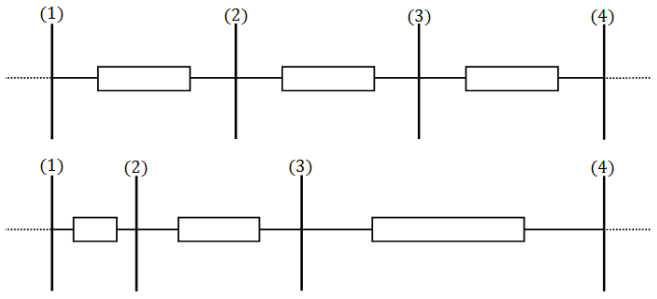

Figure 6. Comparison between the two spacing methods. The bottom bus distribution results in a higher Maximum Common Gain Factor α. The distance between generating busses (1) and (4) are the same for both cases.

These conclusions can also apply for situations where we have more than one DER connected per bus. Though the presence of more than one generator per bus would make it impossible to generalize $[A]$ as a triangular matrix, the busses can still be isolated from one another. Ideally, we would get a situation similar to study model 1 (not shown here), with 3 DERs connected to the same bus, with a Maximum Common Gain Factor $\alpha = 1.6$ instead of 2. The yielded results are indeed applicable for any number of generators (and busses), and their distribution throughout a feeder grid. Dispersing distributed generation has thus a somewhat noteworthy benefit in that it can provide a certain security margin when changing a network's DG profile, as with sufficient (and appropriate) distance between the connecting busses we can assure that decentralized voltage control system remains stable throughout the alteration.

VI. Voltage Error Area Integration

A. *Voltage Error Area Correction*

Throughout the study so far, it was been considered that a feeder's network voltage profile suffers alterations solely as a result of the variation in one or more of the DER's injected power. However, natural fluctuations in the node's voltage (and injected power) will invariably occur, owing to the characteristics of a LV network and a multitude of outside factors, which up until now we've neglected to properly take into consideration when simulating our chosen control algorithm. Likewise, it was also considered that the algorithm operates in both an instantaneous and persistent manner for all DG, not accounting for any sort of time lag in the control process. These indiscriminate influences have the potential to disrupt the algorithm's progression at an inopportune time, particularly when the system is operating with its power coordinates are near any of the imposed limits. Therefore, in the interest of obtaining a more efficient voltage regulation system, an alternate strategy for the voltage control process is proposed.

Thus far, the current algorithm basis its operation on a discrete numerical integration of the error: for each new iteration, the control variable is updated based on the current difference between the state variable and the intended set-point. The former's value is, as such, the linear combination of every previously obtained state variable error, with a set coefficient k_I here corresponding to the controller's power gains their respective nodal voltage. Shifting to a temporal (continuous) basis, the summation in the above expression would be turned into an integral, that is the total area between the voltage error curve and the x-axis, for an equivalent interval of time.

We can use this integral value as the benchmark that'll dictate when a controller "steps in" to regulate the injected power of its DER, as opposed to its continual operation. To that effect, we can make it so that a controller acts upon a voltage deviation only when the integral area surpasses a defined limit A_X. The error would then be estimated from the total area, thus mitigating the concerns that may arise due to the introduction of the aforementioned fluctuations.

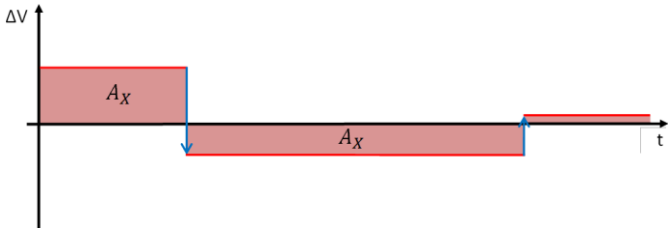

Figure 7. Demonstrative example of an integral voltage error correction over a period of time. The algorithm will act upon the voltage difference only when the darken integral area surpasses a set limit A_X.

Though the area that a controller takes into account is tallied from the last moment the error was zero, given the innately oscillatory behavior of the network's voltage profile, utilizing such average might not be ideal. Because of this and other factors, the calculated mean error might diverge significantly from its actual value at the onset of a power shift. For the sake of a more precise adjustment, we can have the mean error be taken solely from a fixed segment of time directly before the readjustment in the injected power.

Overall, limiting the controllers' intervention on a whole works for the system's benefit, as it avoids unnecessary shifts in active and reactive power that result from oscillations in the nodal voltage. Yet, its most significant advantage is that it practically guarantees that no two generating nodes will vary their injected power simultaneously. As mentioned in Section III, it's the concurrence between the operation of the various controllers that it's at the core of the instability issue for decentralized power control. Assuring that a maximum of one controller i is acting at any given time, then the eigenvalues of $[A]$ will be equal to 1 and $1 - R_{ii}k_{ii} = 1 - \alpha$, considering $[k] = \alpha[R_I]$. The algorithm's convergence is thus guaranteed so long as $0 < \alpha < 2$, regardless of the number of DERs and their configuration throughout the feeder network.

B. *Voltage Error Behavior and System Performance*

Using this new paradigm, we simulated the evolution of the voltage error for the previous study models. We've considered that each controller, upon activation, executes its power adjustment within a millisecond, sampling the last ten milliseconds of the voltage error for reference, with voltage error area set-point of $A_X = 10^{-3}$. Left graphs showcase the error progression without fluctuations, and opposite side with. Under each are the timestamps for the controller's activation.

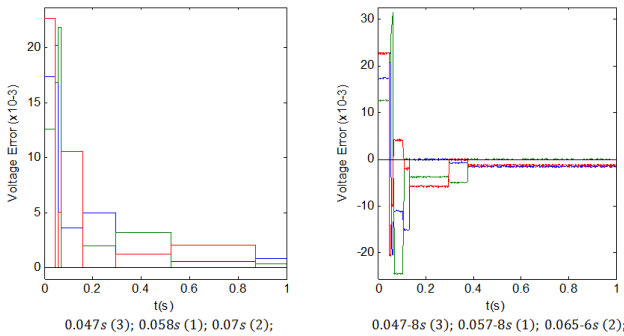

0.047s (3); 0.058s (1); 0.07s (2); 0.160s (3); 0.296s (1); 0.524s (2); 0.875s (3)

0.047-8s (3); 0.057-8s (1); 0.065-6s (2); 0.107s (2); 0.133s (1); 0.299s (2); 0.377s (2)

Figure 8. Evolution of the voltage error for model 6, employing integration of the voltage error area, during a one second interval, with α = 1.*

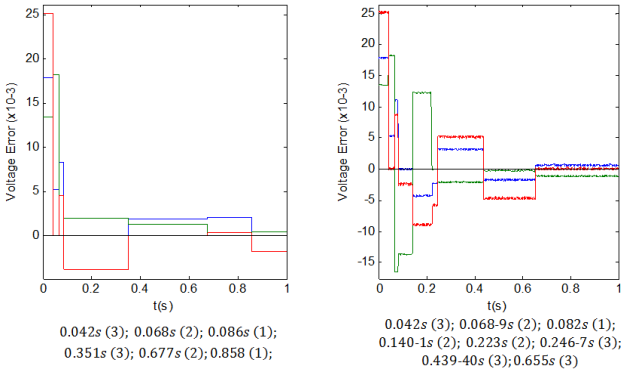

Figure 9. Evolution of the voltage error for model 9, employing integration of the voltage error area, during a one second interval, with $\alpha = 1$.*

*(Note that the right graph on both figures represents only one possible outcome of the error's evolution, due to the randomized nature of the voltage fluctuations.)

As we can observe, although the voltage error does not converge in a manner similar as the examples in Section IV, there's at least a significant reduction in all cases during the presented time interval. Not only that, given the nature of its controllers, this system comes to prioritize the correction of the highest and most lasting discrepancies, another useful trait to have as to safeguard the network's health. Regarding the differences between the left and right sides, the main standout appears to be that the latter is more prone to have larger amplitudes in its "oscillations". At any rate, both sides still manage to achieve a comparable reduction their error.

C. *Dynamic Error Sampling*

The large oscillations on the right come as the result of an deficient estimate on the controller's part. The sampled average error is inferior to the actual error at the onset of its activation, resulting in a shift of the injected power that does not lower (or increase) the nodal voltage past V^* within an allotted time tick. As a consequence, the value of the error integral will not reset, causing the controller to activate again, using roughly the same sampled error as a basis. This effectively results in nodal voltage variation to double.

The simplest workaround would be to ensure that $\alpha > 1$, so that the controller would naturally overcompensate for any possible discrepancies between the sampled and actual error, ensuring that it goes through zero (resetting A_X in the process) within a single tick. However, if α is too low, its effects might end up being negligible, while if it is too high, it may induce more of the same oscillations we're attempting to lessen. Simply reducing the sample period would likewise be a limited scope resolution.

Beyond these small fluctuations, it's again the generators' mutual influence that lies at the heart of the issue. If within a controller's sampling period a change in the nodal voltage were to occur, due to a different controller's activation, then the calculated average will be significantly different than its current error. As such, we can make it so that a controller is able to automatically readjust its sampling period should it detect a large rise or fall in its voltage within a short interval.

Adopting this new sampling methodology, with $\alpha = 1.1$, we repeated the previous set of simulations..

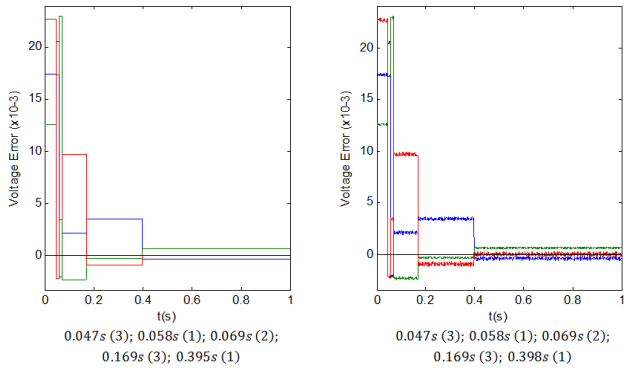

Figure 10. Evolution of the voltage error for model 6, employing integration of the voltage error area with dynamic sampling, during a one second interval.

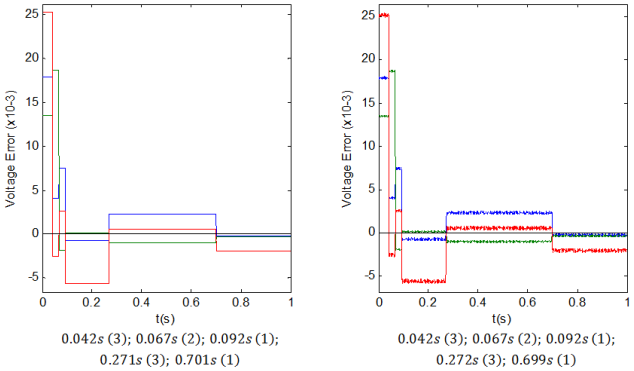

Figure 11. Evolution of the voltage error for model 9, employing integration of the voltage error area with dynamic sampling, during a one second interval.

It's readily obvious that the graphs on opposite sides are nearly identical, a fact that is further hammered in by their near equal timestamps. The error behavior with the added fluctuations also remains more or less consistent, with only a few differences of a couple milliseconds in its timestamps from simulation to simulation. The large error oscillations that cropped up in the previous figures are also, for the most part, eliminated. Thus, it's presumable to say that the effect of these random fluctuations have on the system's error has been effectively lessen, although for relatively small amplitudes only.

VII. Conclusions

As underlined in the introduction, the avowed objective of this work was to propose such a theoretical operable control strategy, that could (in a future instance) be employed by micro-producers to regulate their own operation without the need of oversight from any external entity. Throughout the paper, we've strived to develop a voltage control scheme that could eliminate or minimize the impact of these inherent inadequacies, yielding two results in the form of the Alternating Q(V)/P(V) Controller and the Voltage Error Area Integration Controller.

The results of this thesis demonstrate that implementing a decentralized voltage control strategy for DG in a LV network can indeed be feasible, in theory. Despite the numerous issues that plague it, such as the pervasive threat of instable behavior and lacking performance, it is possible to circumvent them through adequate planning of the controllers' gains and their control algorithm. However, as noted by German military theorist Helmuth von Moltke, *"No battle plan survives contact with the enemy"*. That's to say, when theory is pitted against the real world, the latter will invariably come out on top.

In spite of our efforts to factor in several limiting factors into our calculations and solutions, such as restrictions on injected power and voltage fluctuations, the results obtained throughout this work were still drawn from a simplified scenario rather than a realistic one. And even presented with such model conditions, we've still encountered a significant number of complications, that can prove nonetheless critical to the control system's operation, and possibly a death knell to the near-future widespread adoption of decentralized control strategies. Future, more in-depth and in practice, studies are thus believed to be required to properly gauge the realistic viability of the autonomous option in real-life LV distribution networks. Even so, it's hoped that the provided strategies, even if not viable as practical solutions, can at least serve as a stepping stone towards the formulation of a workable decentralized control scheme.

More importantly, it was our goal throughout the course of this work to draw attention to the inherent limitations of decentralized voltage control, shining a light on a previously poorly studied field of research, and hopefully stimulate a broader discussion within the pertaining academia on the topic.

VIII. References

[1] E. E. P. I. Association, Global Market Outlook for Photovoltaics Until 2014, 2010.

[2] J. Deutch, and E. Steinfeld, "A Duel in the Sun: The Solar Photovoltaics Technology Conflict between China and the United States," in *Report for the MIT Future of Solar Energy Study*. Cambridge, MA, USA: Mass. Inst. Technol., May 2013.

[3] M. Bolen, and F. Hassan, Integration of Distributed Generation in the Power System. Piscataway, NJ, USA: Wiley/IEEE Press, pp. 88, 2011.

[4] C. L. Masters, "Voltage rise: The big issue when connecting embedded generation to long 11 kV overhead lines," *Inst. Elect. Eng. Power Eng. J.*, vol. 16, pp. 5-12, Feb. 2002.

[5] P. F. Ferreira, P. M. S. Carvalho, L. A. F. M. Ferreira, and M. D. Ilic, "Distributed Energy Resources Integration Challenges in Low-Voltage Networks: Voltage Control Limitations and Risk of Cascading," *IEEE Trans. Sustain. Energy*, vol. 4, no. 1, pp. 82–88, Jan. 2013.

[6] M. H. J. Bollen, and A. Sannino, "Voltage control with inverter-based distributed generation," *IEEE Trans. Power Del.*, vol. 20, no. 1, pp. 519–520, Jan. 2005.

[7] C. M. Hird, H. Leite, N. Jenkins, and H. Li, "Network voltage controller for distributed generation," *Proc. Inst. Elect. Eng., Gen., Transm., Distrib.*, vol. 151, no. 2, pp. 150–156, Mar. 2004.

[8] A. E. Kiprakis, and A. R. Wallace, "Maximizing energy capture from distributed generators in weak networks," *Proc. Inst. Elect. Eng., Gen., Transm., Distrib.*, vol. 152, no. 5, pp. 611–618, Sep. 2004.

[9] P. M. S. Carvalho, Pedro F. Correia, and Luís A. F. M. Ferreira, "Distributed Reactive Power Generation Control for Voltage Rise Mitigation in Distribution Networks," *IEEE Trans. On Power Systems*, vol. 23, no. 2, pp. 766–772, May 2008.

[10] P. M. S. Carvalho, L. A. F. M. Ferreira, and J. J. E. Santana. "Single-Phase Generation Headroom in Low-Voltage Distribution Networks Under Reduced Circuit Characterization," *IEEE Trans. Power Systems*, vol. 30, no. 2, pp. 1006-1011, Mar. 2015.